3084–3091 Nucleic Acids Research, 1994, Vol. 22, No. 15 

# Heat shock affects 5′ splice site selection, cleavage and ligation of CAD pre-mRNA in hamster cells, but not its packaging in InRNP particles

Elana Miriami, Joseph Sperling[1] and Ruth Sperling*
Department of Genetics, The Hebrew University of Jerusalem, Givat Ram, Jerusalem 91904 and
[1]Department of Organic Chemistry, The Weizmann Institute of Science, Rehovot 76100, Israel

Received April 29, 1994; Revised and Accepted June 20, 1994

## ABSTRACT

**The effect of heat shock on the packaging and splicing of nuclear CAD pre-mRNA, a transcript expressed constitutively from a non heat-inducible promoter, was studied *in vivo* in Syrian hamster cells. While mild heat shock did not affect significantly the packaging of CAD RNA in 200S InRNP particles, it caused perturbation to splicing. First, the heat shock inhibited splicing of CAD pre-mRNA. Second, it affected 5′ splice site selection by activating cleavage at a cryptic 5′ splice site; yet ligation of the cryptic exon to the downstream proximal exon was not observed. Base complementarities of the cryptic site with U1, U5, or U6 snRNAs are comparable, or even better, than those with the neighboring normal site. Hence, the exclusion of the cryptic site under normal growth conditions cannot be attributed to weaker base pairing with these snRNAs. On the other hand, these results imply the involvement of a heat labile factor in the selection of the 5′ cleavage site. The exclusion of the cryptic site at 37°C and the aborted splicing at this site after heat shock may also be explained by a proposed nuclear checking mechanism that detects in-frame stop codons upstream of the 5′ splice site, and aborts splicing at such sites to prevent the production of a defective message.**

## INTRODUCTION

The maturation of most eukaryotic precursor messenger RNA (pre-mRNA) involves the removal of intervening RNA sequences by two transesterification reactions (reviewed in 1–3). The first entails cleavage at the 5′-splice site with the concomitant formation of a 2′-5′ phosphodiester bond between the 5′ terminal guanosine residue of the intron and an adenosine residue located approximately 30 nucleotides upstream from the 3′-splice site. The second step involves cleavage at the 3′-splice site, ligation of the two exons and release of the excised intron in a lariat form. *In vitro*, splicing reactions occur only after the assembly of a multicomponent ribonucleoprotein (RNP) complex which is termed the spliceosome [reviewed in (1–4)].

The accuracy of splice site selection and the efficiency of the cleavage and ligation reactions have been attributed to base pairing interactions between conserved pre-mRNA and U snRNA sequences. Base pairing interaction between the 5′ end of U1 snRNA and conserved sequences flanking the splice sites in the pre-mRNA is required for the subsequent assembly of a functional spliceosome (1,4–8), and has been implicated in the mechanism for 5′-splice site selection (9,10).

Experiments using pre-mRNA with duplicated 5′-splice sites have suggested that neighboring potential 5′-splice site sequences can be ranked in a hierarchy of preferential usage. The intrinsic strength of a splice site sequence is related to its degree of resemblance to the consensus sequence (11–14). However, not all pre-mRNA sequences that conform to splice junction consensus sequences are selected for splicing (1,14,15). This indicates that additional interactions are required for accurate 5′-splice site selection. In addition, Séraphin and Rosbash (7) have shown that exon mutations uncouple 5′-splice site selection from U1 snRNA pairing, suggesting that the requirements for 5′-splice site selection and cleavage are different. Recent studies have suggested that 5′-splice site selection involves several steps, in which U1, U5, and U6 snRNPs participate, before the first cleavage actually occurs (16–19).

In severely stressed cells, RNA processing is inhibited. This was first described by Yost and Lindquist (20) who showed that the maturation of heat shock protein (hsp) 82, which is expressed from an intron-containing gene, is significantly reduced in severely heat shocked Drosophila melanogaster Schneider cells. This was accompanied by the accumulation of full length precursor RNA. Other Drosophila hsp genes do not contain introns, and therefore their expression is not affected. The block in splicing is not limited to hsp 82 transcripts, as heat shock also prevents splicing of transcripts from non-heat shock genes expressed under a heat shock promoter (20,21). Inhibition of splicing has also been demonstrated in other organisms (22–26). The precise nature of the block in splicing is not known. Yet, since full length precursor accumulates (in hsp 82, for example), it has been suggested that the block occurs early in the splicing pathway (27).

*To whom correspondence should be addressed

In previous studies we have shown that nuclear RNP complexes of several specific transcripts that vary largely in size, can be released from the nuclei of mammalian cells as large particles that invariably sediment at the 200S region in sucrose gradients (28,29). We have further shown that practically all nuclear polyadenylated RNA is packaged in these large nuclear RNP (lnRNP) particles (28). In addition to RNA, the lnRNP particles consist of a multitude of proteins, including an essential splicing factor (30), and the U1, U2, U4, U5 and U6 snRNP complexes that are essential for splicing (31,32, and Miriami and Sperling, in preparation). Electron microscopy reveals compact particles, with a diameter of 50 nm (28), that are similar to RNP particles visualized *in situ* (32). These studies have led us to suggest that the lnRNP particles faithfully represent the native RNP complexes on which RNA processing occurs *in vivo* (32).

To study the effect of heat shock on the splicing of a multi-intron constitutive gene product, and on its packaging in an lnRNP complex, we have employed the CAD lnRNP system (28,29,31). The CAD gene (abbreviated for the multifunctional enzyme carbamoyl-phosphate synthetase, aspartate trans-carbamylase, and dihydro-orotase) is expressed from a non heat inducible promoter (33). Here we report that heat shock treatment of Syrian hamster cells causes disruption of CAD pre-mRNA splicing. First, it inhibits splicing of CAD pre-mRNA. Second, it affects splice site selection by promoting cleavage at a cryptic consensus splice site sequence. However, heat treatment has no apparent effect on the general mode of packaging of the accumulated precursors and the cryptic cleavage product, all of which sediment as 200S lnRNP particles.

## MATERIALS AND METHODS

### Cells

Syrian hamster PALA-resistant cells [line 165−28, (34), kindly provided by G.R.Stark] were grown at 37°C in 8 cm petri dishes as described (29). For heat treatment, the plates were wrapped with parafilm and incubated in a water bath shaker at 43°C or 45°C (± 0.2°C) for the specified length of time.

### Plasmids and probes

PGS—a subgenomic clone of CAD DNA—was prepared from the genomic clone $pCAD_{142}$ (35) (kindly provided by G.R.Stark) by subcloning a 977 bp SalI−PstI fragment into pGEM4 at the appropriate sites (Kahana and Sperling, unpublished). To prepare the 3′ end-labeled CAD genomic probe, the plasmid was digested with SalI (Figure 1A), and labeled with [$\alpha$-$^{32}$P]dCTP and [$\alpha$-$^{32}$P]dTTP in the presence of Klenow polymerase. To prepare the 5′ end-labeled probe, PGS was digested with AccI (Figure 3A), treated with calf intestine alkaline phosphatase, and labeled with [$\gamma$-$^{32}$P]ATP in the presence of T4 polynucleotide kinase.

### Cell fractionation and nuclear RNP preparation

Nuclear and cytoplasmic fractions of Syrian hamster cells were prepared as described previously (28) except that $\beta$-mercaptoethanol was omitted from all buffers. Nuclear supernatant was prepared from the purified nuclei by mild sonication and precipitation of chromatin, and was fractionated in a 15−45% sucrose gradient to give 200S lnRNP particles (29,31).

### RNA preparation

RNA was recovered from cytoplasmic-, nuclear-, or gradient-fractions by the addition of SDS to 1%, yeast tRNA to 50 $\mu$g/ml, incubation with 200 $\mu$g/ml proteinase K for 30 min at 37°C, phenol extraction and ethanol precipitation. Total cellular RNA was extracted with guanidinium thiocyanate (36) and the RNA was purified by sedimentation through a CsCl cushion using a modified protocol described by Sperling *et al.* (29).

### S1 nuclease mapping of CAD RNA

Typically, RNA samples of 10 to 100 $\mu$g were hybridized at 56°C for 24 hr with 50 ng of the appropriate $^{32}$P-labeled CAD probe ($10^7$ cpm/$\mu$g) and digested with S1 nuclease (500−1000 u/ml) at 43°C for 30 min. The protected DNA fragments were denatured in 80% formamide at 95°C for 3 min and analyzed by electrophoresis in 4.5% or 6% polyacrylamide/7 M urea gels and autoradiography. As controls, samples were analyzed in the absence of added RNA.

### RNA−PCR assay

Prior to reverse transcription, the RNA was treated with 50 u/ml RQ1 DNase (Promega) in the presence of 500 u/ml RNasin at 37°C for 10 min and recovered by proteinase K digestion, phenol extraction and ethanol precipitation. Following this DNase treatment, and in the absence of reverse transcriptase, no amplified product was detectable.

cDNA molecules were prepared from the RNA samples by reversed transcription using the cDNA cycle kit for RT−PCR (Invitrogen) according to the manufacturer's instructions.

The following CAD PCR primers were used:

Primer a: [+] 5′ CCGGGTGCAGGAGTGACAGC 3′;
Primer b: [+] 5′ CTCCAGAGGCGGAGAGGCCC 3′;
Primer c: [−] 5′ CAGGAGCCGCACCAGTTTC 3′;
Primer d: [+] 5′ CCAAACTCTTCGTGGAGGCCC 3′.

PCR reactions (25−35 cycles) in the DNA Thermal Cycler (Perkin-Elmer) were performed using Taq DNA polymerase (Boehringer; 0.5 u/reaction) and 10 pmole each of the noted primer pairs (Figure 4A) as follows: denaturation at 95°C for 1.5 min; annealing at 60°C for 1.5 min; synthesis at 72°C for 1.5 min (7 min for the last cycle). The amplification products were analyzed by electrophoresis in 1.6% agarose gel.

### Protein dot blot analysis

Aliquots of 5−10 $\mu$l from each gradient fraction of RNP particles were spotted onto a nitrocellulose membrane. The membrane was blocked with 10% low-fat milk in PBS containing 0.1% Triton X100 for 1 hr at 25°C and incubated with the appropriate antibodies (diluted in PBS/0.1% Triton X100 as indicated) for 1 hr at 25°C. The membrane was washed five times for 10 min with wash buffer (0.25% low-fat milk in PBS/0.1% Triton X100) and incubated for 1 hr at 25°C with horseradish peroxidase linked to protein A or with sheep anti-human Ig horseradish peroxidase linked F(ab′) 2 fragment (Amersham) diluted 1:3000 or 1:1000, respectively in wash buffer. The blots were washed with wash buffer and the antibodies were detected with the ECL immunofluorescence kit (Amersham) according to the manufacturer's manual.

### Electron microscopy

Aliquots from the 200S peak fraction of the sucrose gradient were negatively stained with 1% uranyl acetate and visualized by electron microscopy as previously described (28).

## RESULTS

### Heat shock specific CAD RNA products

Precursor and mature CAD RNA molecules formed *in vivo* in Syrian hamster cells were analyzed by S1 mapping of total cellular RNA using a 3′-end labeled subgenomic CAD probe. This S1 mapping strategy allows a simultaneous analysis of all splicing intermediates in a region of four exons and three introns, independently of the splicing state at all other regions of the 25 kb CAD RNA transcript which contains 37 introns.

The expected splicing intermediates and products are shown schematically in Figure 1A. The following RNA species were identified in cells grown at 37°C (Figure 1B): (i) Mature RNA is represented by the predominant band of 105 nucleotides (nt), that arose mainly from protection of the probe by RNA species from which intron 1 (IVS1) had been spliced. The contribution to this fragment of RNA species that had only been cleaved at the 5′ splice site of IVS1 was low (see text describing Figure 3B); (ii) Pre-mRNA is represented by the 972 nt band, that arose from full protection of the probe; (iii) The intermediate species

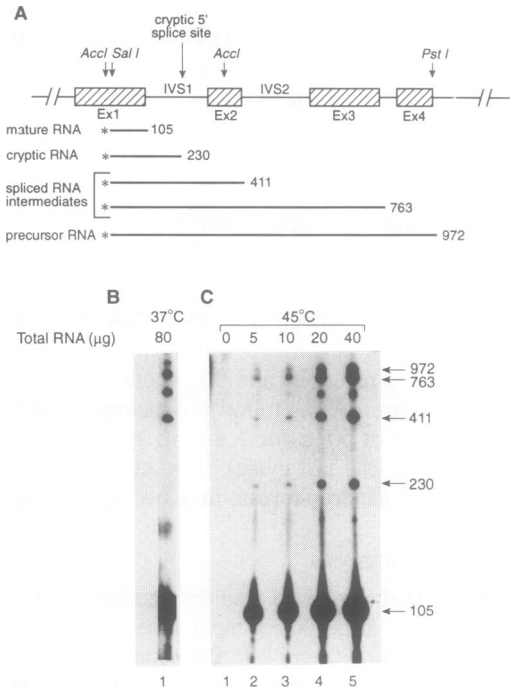


**Figure 1.** A heat shock specific CAD RNA product. (**A**) Map of the SalI−PstI CAD genomic DNA probe and the expected 3′ end labeled DNA fragments protected by CAD pre-mRNA, splicing intermediates, and products after S1 mapping analysis (the numbering of exons [Ex] and introns [IVS] refer to the subgenomic fragment). (**B, C**) Nuclease S1 mapping analysis of total CAD RNA from cells grown at 37°C (B), and from cells heat treated for 30 min at 45°C (C). The indicated amounts of total RNA were hybridized with the 3′ end labeled probe and digested with nuclease S1. The labeled protected DNA fragments were analyzed by electrophoresis on denaturing gels. A 230 nt fragment is observed only after heat shock.

in this multi-intron system are represented by the 411 and the 763 nt bands that arose from protection by RNA molecules cleaved (or spliced) at the exon 2-IVS2 and exon 3-IVS3 splice junctions, respectively. The 600 nt band may have arisen from DNA−DNA hybrids, as this band was sometimes observed in S1 analyses with no added RNA (not shown), while the other bands were seen only in the presence of RNA.

Analysis of RNA from cells subjected to heat shock at 45°C for 30 min revealed a new protected band of 230 nt, whose intensity increased linearly with the increase in the amount of total RNA used in the assay (Figure 1C, lanes 2−5). The 230 nt fragment arose from protection of the probe by RNA species cut within IVS1. Sequence data have confirmed that the 3′ end of the 230 nt fragment maps to a cryptic consensus 5′ splice site within IVS1 (see below).

### The cryptic-, precursor- and spliced intermediates CAD RNAs are localized in the nucleus

S1 mapping was carried out on nuclear and cytoplasmic RNA fractions isolated from cells before and after heat treatment at 43°C or 45°C for various lengths of time (Figure 2A and 2B). Mature CAD RNA, corresponding to the 105 nt fragment, was observed in the nuclear and cytoplasmic fractions. It should be noted, that the abundance of mature CAD RNA in the nuclei of cells grown at 37°C has been confirmed previously (29). The pre-mRNA and partially spliced intermediate molecules, represented by the 973, 763 and 411 nt fragments, were observed only in the nuclear-, but not in the cytoplasmic RNA fractions of both heat-treated and untreated cells (Figure 2A and 2B, compare lanes marked Nuc and Cyt). The cryptic RNA product, corresponding to the 230 nt fragment, was found only in the nuclei of heat-treated cells (Figure 2A and 2B, compare lanes marked Nuc in the 37°C panel to those marked Nuc in the 43°C or 45°C panels). A second cryptic protected product of 200 nt was detected in the nuclear fraction after 45 and 60 min of treatment at 45°C. This fragment corresponds to a cleavage product at an additional cryptic consensus 5′ splice site sequence within IVS1 (Figure 2B). Notably, the pre-mRNA, spliced intermediates and cryptic CAD RNA molecules were confined to the nucleus even after recovery from heat shock at 37°C for 2 hr (data not shown). The confinement of these CAD RNA species to the nucleus was confirmed by using higher input levels of RNA and longer exposures of the gels.

The steady state amounts of CAD RNAs were different in heat shocked cells than in cells grown at 37°C (Figure 2). The patterns of CAD RNA accumulation during incubation of the cells at 43°C or at 45°C were qualitatively similar, with some quantitative differences (Figure 2). The heat shock specific 230 nt product reached maximal levels at 30 min of heat treatment and decreased during continued heat shock. It reached a greater maximal value during incubation at 43°C than during incubation at 45°C. The 763 and 411 nt fragments reached the same maximal levels after 15 min of heat treatment (Figure 2A, lanes 6, 7; Figure 2B, lanes 1, 2). However, they accumulated to a greater extent at 45°C than at 43°C. The levels of these species also decreased with continued heat treatment. The full-length precursor, represented by the 972 nt fragment, accumulated to a much greater extent upon heat shock at 45°C than upon incubation at 37°C or 43°C.

Inhibition of splicing is possibly the major cause for the initial burst in the amount of pre-mRNA and spliced intermediates in heat-stressed cells. However, the subsequent decay of these-, and the decay of the heat shock specific cryptic RNA species (Figure

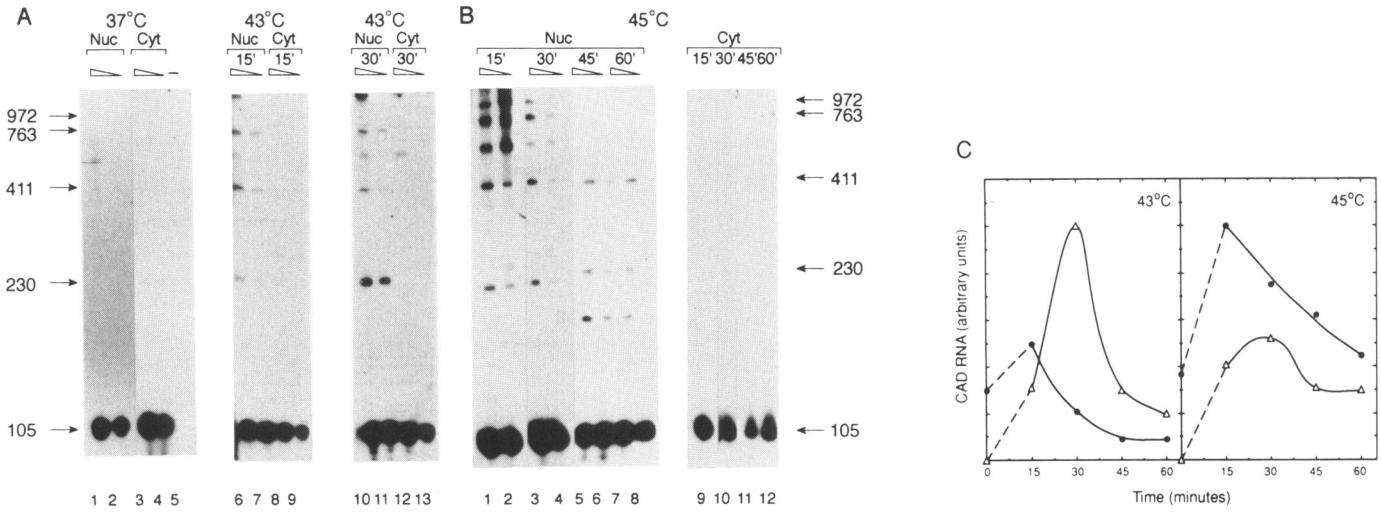


**Figure 2.** Nuclear accumulation of CAD pre-mRNA and spliced intermediates in heat shocked cells. Nuclear (Nuc) and cytoplasmic (Cyt) RNAs were isolated from cells grown at 37°C and from cells heat treated as indicated. The RNA was analyzed by S1 mapping using the 3'-end labeled probe as described in Figure 1. (**A**) Nuclear and cytoplasmic RNAs from $2\times10^6$ cells (lanes 2, 4, 7, 9, 11, 13) and from $4\times10^6$ cells (lanes 1, 3, 6, 8, 10, 12). Lane 5, control without RNA. (**B**) Nuclear and cytoplasmic RNAs from $4\times10^6$ cells (lanes 1, 3, 5, 7, 9–12) and from $2\times10^6$ cells (lanes 2, 4, 6, 8). (**C**) Time course of the accumulation and decay of the cryptic CAD RNA product represented by the 230 nt protected fragment (Δ), and of the spliced CAD RNA intermediates represented by the 411 nt protected fragment (●), upon heat treatment at 43°C (left panel) and 45°C (right panel). The data was taken from Figure 2A and 2B, and from additional experiments not shown. The time point at the origin is for cells grown at 37°C.

2C) suggest that additional heat-induced changes, affecting the general stability of RNA and/or its rate of transcription, become dominant at prolonged heat treatment. Therefore, further experiments were performed with cells that had been heat treated for 15 or 30 min only.

### Ligation at the cryptic splice site is blocked

To determine whether ligation at the cryptic site was affected by heat-treatment, we performed S1 nuclease mapping with a 5′ end-labeled subgenomic probe cut with AccI at exon 1 and exon 2. The splicing intermediates and splicing products expected from splicing between these two exons are shown schematically in Figure 3A. The following RNA species were identified in cells grown at 37°C (Figure 3B lanes 1, 2): (i) Mature RNA is represented by the predominant band of 46 nt. (ii) Pre-mRNA is represented by the 376 nt band. The 376 nt fragment arose from full protection of the probe and corresponds to all precursor and partially spliced CAD RNA molecules that had intact IVS1. (iii) The IVS1−Ex2 intermediate is represented by the 270 nt band. The 270 nt fragment arose from protection of the probe by RNA species cleaved at the normal 5′ splice-site, and it corresponds to the steady state population of RNA molecules that had completed only the first step of splicing at this site. The intensity of the 5′ end labeled 270 nt band (Figure 3B lane 1) is extremely low with respect to the 3′ end labeled 105 nt band (Figure 3B lane 7), which represents the combined populations of spliced Ex1−Ex2 and free Ex1. Because both lanes were loaded with equivalent amounts of material, it can be concluded that the steady state population of free Ex1 is extremely low with respect to that of Ex1−Ex2.

Analysis of RNA from nuclei of cells heat-treated at 43°C for 30 min revealed a new specific band of 145 nt (Figure 3B, lanes 3 and 4). The 145 nt fragment arose from protection of the probe by RNA species cut within IVS1 at a cryptic 5′-splice site, and represents a cryptic IVS1−Ex2 intermediate. The 3′ end of the 145 nt fragment (defined by the 5′ end labeled probe) and the 5′ end of the 230 nt fragment (defined by the 3′ end labeled probe) map to the same site. Moreover, the intensity of the 145 nt band (Figure 3B, lane 3) is very similar to that of the 230 nt fragment (Figure 3B, lane 8). Thus, it can be concluded that both fragments originated from cleavage at the same (cryptic) site. The similar intensities of the 230-, and the 145 nt bands also indicates that ligation of cryptic exon 1 (Ex1* in Figure 4A) to Ex2 did not occur. However, this S1 mapping experiment does not allow to determine whether the 3′ end of Ex1* RNA remained free, or whether it underwent ligation to a 3′ splice site downstream of Ex2. The second possibility is highly unlikely since the 230 nt is confined to the nuclear fraction and excluded from the cytoplasmic one, indicating that there was no ligation of Ex1* to any downstream exon with the production of stable mRNA that would accumulate in the cytoplasm.

To confirm that ligation of cryptic exon 1* to exon 2 did not occur we used PCR to look for the aberrant mRNA that would arise from this ligation. PCR was performed on cDNA prepared from nuclear and cytoplasmic RNA fractions that were isolated from cells before and after heat-treatment at 43°C for 30 min. The sets of primers and the expected PCR products are shown schematically in Figure 4A. The primers used were: Primer a, a 20-base oligonucleotide from a sequence within IVS1 upstream of the cryptic cleavage site; Primer b, a chimeric oligonucleotide consisting of 16 bases immediately upstream of the cryptic cleavage site plus the first 4 bases of exon 2, covering the expected splice-junction between Ex1* and Ex2; Primer c, a 19-base oligonucleotide from the 3′ end of exon 2; Primer d, a chimeric oligonucleotide consisting of 17 bases immediately upstream of the normal 5′ cleavage site of exon 1 plus the first 4 bases of exon 2, covering the splice junction between Ex1 and Ex2.

If Ex1* and Ex2 were ligated to each other, we expected to see the following products at 43°C: Using primers a and c, we

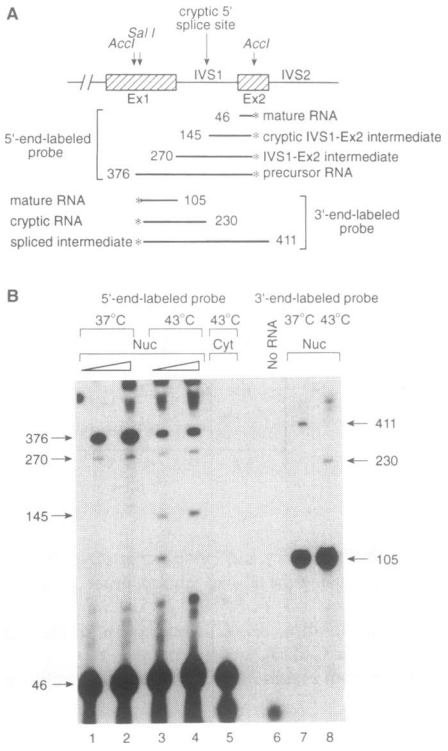


**Figure 3.** Nuclear accumulation of cryptic splicing intermediates after heat shock. (**A**) Map of the AccI fragment of the CAD subgenomic probe and the protected 5′ end labeled DNA fragments expected from CAD pre-mRNA and splicing intermediates after nuclease S1 mapping analysis. The protected DNA fragments expected from this region utilizing the 3′ end labeled probe are shown for comparison. (**B**) Nuclear and cytoplasmic RNAs were prepared from cells grown at 37°C and from cells heat treated for 30 min at 43°C. The RNA was analyzed by nuclease S1 mapping as described in Figure 1, using the 5′ end labeled probe (lanes 1–6) or the 3′ end labeled probe (lanes 7, 8) for comparison. The amounts of RNA used were from: $4\times10^6$ cells in lanes 1, 3, 6, 7, 8; $8\times10^6$ cells in lanes 2, 4; and none in lane 6 as a control. Heat treatment at 43°C for 30 min was chosen since the level of cleavage at the cryptic 5′ splice site was maximal at this time point. The levels of the pre-mRNA and splicing intermediates, represented by the 5′ end labeled 376 and 270 nt protected fragments, was maximal after 15 min of heat treatment (data not shown), confirming the results obtained with the 3′ end labeled probe (Figure 2).

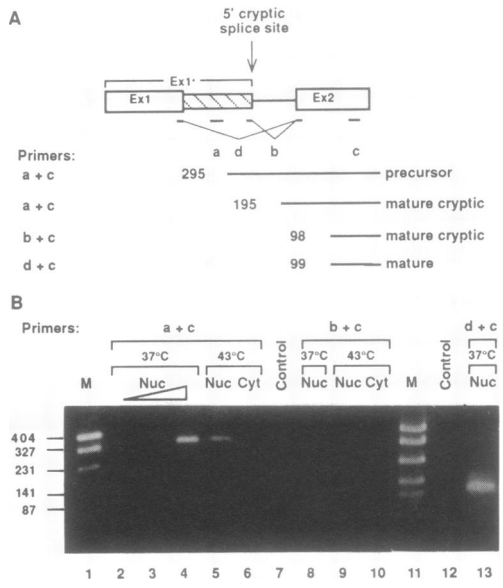


**Figure 4.** RNA PCR amplification shows that splicing at the cryptic site is blocked at the second step. (**A**) Schematic map of CAD RNA flanking the cryptic 5′ splice site and the PCR products expected from the indicated pairs of primers. (**B**) cDNA prepared from nuclear and cytoplasmic RNAs isolated from cells that had been grown at 37°C and from cells heat treated at 43°C for 30 min, was subjected to PCR amplification (30 cycles), using the pairs of primers as indicated. Lanes 1 and 11, size markers of $\phi$X174 DNA cut with TaqI; lanes 2–4, analyses of RNA from $5\times10^4$, $10^5$, and $5\times10^5$ cells, respectively; lanes 5–10, analyses of RNA from $10^5$ cells; lanes 7 and 12, (control) PCR amplification without reverse transcription using nuclear RNA from cells treated at 43°C for 30 min (no PCR products were detected); lane 13, analysis of RNA from $10^5$ cells. (No products representing cryptic mRNA were obtained even after 35 cycles of amplification).

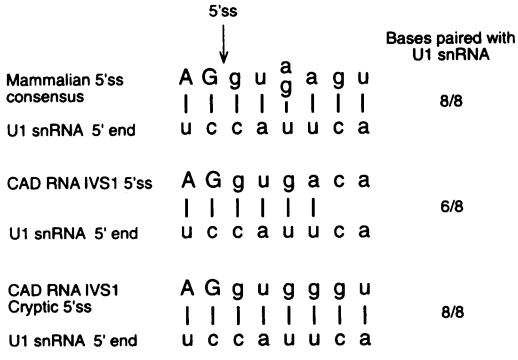


**Figure 5.** The sequence at the 5′ cryptic splice site is a consensus sequence that can base pair with U1 snRNA. CAD pre-mRNA sequences at the normal 5′ splice site of exon 1 and at the downstream cryptic 5′ splice site are presented, and complementarity with the conserved 5′ end of U1 snRNA is shown. (Exon sequences, upper case letters; intron sequences and U1 sequences, lower case letters).

expected to see the 295 nt fragment representing the pre-mRNA, as well as an aberrant mRNA PCR product of 195 nt. Using primers b and c, we expected to see only the aberrant mRNA product, which in this case would be 98 nucleotides long. If Ex1* and Ex2 could not be ligated together then only the 295 nt PCR product resulting from pre-mRNA would be detected, and then only with primers a and c.

As expected, primers a and c gave rise to the 295 nt pre-mRNA product only in the nuclear RNA fractions of cells—whether grown at 37°C or heat treated at 43°C (Figure 4B, lanes 4 and 5, respectively). Notably, however, neither primers a and c, nor primers b and c, gave rise to the respective PCR products representing aberrant mRNA (Figure 4B, lanes 5, 6 and 9, 10, respectively). As a positive control we used the chimeric primer d with primer c to demonstrate that under the conditions used here for the PCR reactions a 99-nt PCR product, expected from normally ligated Ex1–Ex2, was obtained (Figure 4B, lane 13). We conclude that due to heat treatment cleavage occurs at the 5′ cryptic site, but ligation at this site is apparently blocked. Products of this cryptic cleavage event accumulate as reaction intermediates, i.e., as free 5′ Ex1* and the cryptic IVS1–Ex2 intermediate. Yet, products representing spliced Ex1*–Ex2 were not observed.

## The cryptic 5′ splice-site is a consensus sequence

To see whether the exclusion of the use of the cryptic site under normal growth conditions could be due to mispairing between

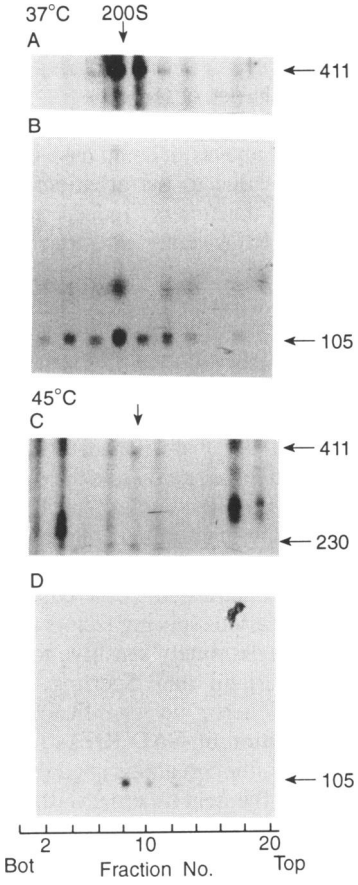


**Figure 6.** Heat treatment does not affect the packaging of CAD pre-mRNA and splicing intermediates in 200S lnRNP particles. Nuclear RNP particles, prepared from Syrian hamster cells grown at 37°C (panels **A** and **B**) or after heat treatment at 45°C for 15 min (panels **C** and **D**), were fractionated on a 15–45% sucrose gradient. RNA was extracted from each fraction and analyzed by S1 mapping, as described in Figure 1, utilizing the 3′ end labeled probe. Panels A and C, distribution of RNP particles of spliced CAD RNA intermediates and the cryptic cleavage product (only in panel C). Panels B and D, distribution of mature CAD RNP particles. Panel A was obtained by over exposure (14 d) of the upper part of the gel shown in panel B, which was exposed for 20 hr. Panel C was obtained by over exposure (2 d) of the upper part of the gel shown in panel D, which was exposed for 6 hr. The peak fraction of tobacco mosaic virus (TMV), used as a marker for the 200S region, was in fraction 8 of a parallel gradient.

the 5′ cryptic splice-site and U1 snRNA, we examined the sequence of the genomic CAD DNA (Kahana and Sperling, unpublished). The sequence at the cryptic cleavage site (Figure 5) agrees with the consensus sequence for 5′-splice sites (reviewed in 1). The sequence suggests that the cryptic site ought to be able to base pair with U1 snRNA and serve as a legitimate 5′ splice site. In fact, the complementarity between U1 snRNA and the cryptic site is even better than the complementarity between U1 snRNA and the normal 5′ splice-site (Figure 5). Nonetheless, the cryptic site is not selected under normal growth conditions and only after heat treatment is there cleavage at this site. This suggests first, that the splice-site is not selected on the basis of primary sequence alone, and second, that the block in splicing is not due the mispairing between U1 snRNA and the cryptic site. It appears that other factor(s) participate in the choice of the correct splice site.

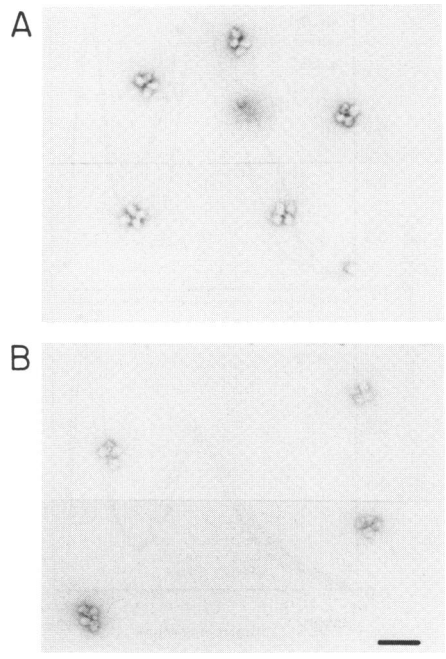


**Figure 7.** Electron micrographs of lnRNP particles. Electron micrographs of particles from the 200S peak of fractionated lnRNPs released from Syrian hamster cells grown at 37°C (**A**) and after heat shock at 45°C for 15 min (**B**). Bar = 100 nm.

## Cryptic-, precursor- and mature CAD RNA are packaged in the 200S lnRNP particles

To test whether heat-shock affects the integrity of the nuclear CAD RNP complex, we compared the distribution in sucrose gradients of nuclear CAD RNP prepared from heat-treated and untreated cells. CAD RNP was released from nuclei of cells before and after heat-treatment at 45°C for 15 min. The distribution of CAD RNA across a sucrose gradient was analyzed by S1 mapping with a 3′ end labeled probe (Figure 6). The mature CAD RNA, represented by the 105 nt fragment (Figure 6B, tubes 8–10), and the spliced intermediate, represented by the 411 nt fragment (Figure 6A, tubes 8–10), were located in the 200S region, as shown previously for mature CAD RNA and additional specific transcripts (28,29,31,32). Heat treatment did not affect the distribution of CAD RNA (Figure 6D, and Figure 6C, tubes 8–10). Furthermore, after heat-shock, the RNA cleaved at the cryptic site, represented by the 230 nt fragment, was also found in the 200S region. It should be pointed out that the level of precursor molecules was higher at 45°C than at 37°C as a several-fold longer exposure time was required to observe the precursor molecules at 37°C.

Electron microscopy of negatively stained lnRNP particles isolated from cells that had been treated at 45°C for 15 min show compact composite structures with a cross section of ~50 nm (Figure 7B). These are similar to the structures obtained for lnRNP particles isolated from cells grown at 37°C (Figure 7A and ref. (28). These results suggest that heat-treatment does not cause major structural changes in the lnRNP particles.

## Heat shock does not affect the distribution of the Sm antigen and a splicing protein in sucrose gradients

We examined whether the distributions across the sucrose gradient of the essential splicing factor SF53/4 (30) and the Sm

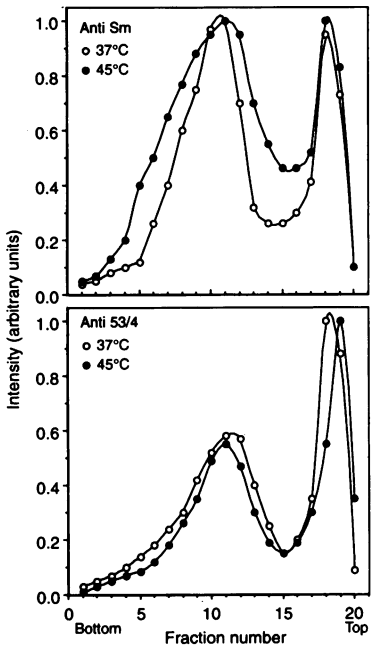


**Figure 8.** The distribution of splicing proteins in nuclear RNP particles is not affected by heat shock. lnRNP particles from cells grown at 37°C and after heat shock at 45°C for 15 min were fractionated on 15–45% sucrose gradients as described. Aliquots from each fraction were spotted onto a nitrocellulose filter, treated with the first antibody (anti-Sm, at 1:50 dilution; MAb 53/4, at 1:400 dilution), and visualized by fluorescence. The quantitation of splicing proteins was done by densitometry and is given in arbitrary units. Upper panel, Sm proteins in lnRNP particles from cells grown at 37°C (○), and from cells treated at 45°C for 15 min (●). Lower panel, splicing factor 53/4 (SF53/4) in lnRNP particles from cells grown at 37°C (○), and from cells treated at 45°C for 15 min (●). The peak of TMV, used as a sedimentation marker, was in fraction 11 of a parallel gradient.

antigen [which is common to all U snRNPs required for splicing (4,37)] were affected by heat-shock. SF53/4 (Figure 8, lower panel) and the Sm antigen (Figure 8, upper panel) are located in two main regions, namely, the 200S and the top of the gradient (the top of the gradient may represent free proteins not associated with the RNP particles). This suggests that the mode of packaging of proteins into lnRNP particles is not changed by heat-shock. This is in agreement with our observation that all five U snRNPs required for splicing are found with the 200S lnRNP particles before and after heat treatment (data not shown).

## DISCUSSION

Previous studies have shown that pre-mRNA splicing *in vivo* is inhibited in a variety of cells treated by heat shock (20–25,27,38), as well as in nuclear extracts prepared from heat-shocked cells (26). Here we investigated the effect of heat treatment on the splicing of the multi-intron CAD pre-mRNA, which is expressed constitutively in Syrian hamster cells from a non heat-induced promoter (33), and on its packaging in lnRNP particles (28,29,32). In accordance with previous reports, we have found that heat shock causes inhibition of normal splicing, as evidenced by the initial burst in the levels of CAD pre-mRNA and spliced intermediates thereof. However, splicing of CAD pre-mRNA in heat shocked cells is disrupted in two additional ways. First, heat treatment affects 5′ splice site selection by activating cleavage at a cryptic consensus sequence that is not utilized under normal growth conditions. Second, completion of splicing at the cryptic site, i.e. second cleavage and ligation to the proximal 3′ exon, is not observed.

Since full-length pre-mRNAs accumulate in heat treated cells (21,23, and results cited above), it could have been expected that the block in splicing is due to perturbations in the assembly pathway of the splicing machinery. Indeed, it has been shown that exogenous pre-mRNA does not assemble into active spliceosomes when added *in vitro* to a nuclear extract prepared from heat treated HeLa cells (26,39,40). However, the reports regarding the situation *in vivo* are conflicting. Mayrand and Pederson (41) observed alterations in the protein to RNA ratio in the general population of RNP particles from heat treated Drosophila and HeLa cells; whereas Kloetzel and coworkers reported that RNP particles were not affected (42,43).

The criteria we have used here to assess the effect of heat shock on general and specific lnRNP complexes include sedimentation in a sucrose gradient and visualization in the electron microscope. In a parallel study we observed that the structural integrity of the lnRNP particles, as manifested by the cosedimentation with specific pre-mRNAs of various splicing factors and the U snRNPs required for splicing, is extremely sensitive to the physical and ionic environment (Miriami and Sperling, in preparation). However, as reported here, no significant differences are observed in the distribution of CAD RNAs (precursor as well as spliced intermediates), the Sm antigen and the SF53/4 splicing factor, before and after the heat treatment—they all cosediment at the 200S region in the sucrose gradient. Furthermore, even the products of the heat shock-induced cleavage at the cryptic site remain packaged in 200S lnRNP particles. Finally, visualization in the electron microscope does not reveal significant morphological differences in lnRNP particles before and after heat treatment. Thus, while splicing is severely impaired, the packaging of CAD pre-mRNA in lnRNP particles appears not to be affected by short heat shock.

The heat-induced activation of cleavage at a cryptic splice site within an intron is intriguing. This cryptic splice site is a consensus sequence with better complementarity with the conserved 5′ end of U1 snRNA than the regular 5′ splice site (Figure 5), yet, splicing at the cryptic site does not occur under normal growth conditions. This observation indicates that base pairing with U1 snRNA is not sufficient for the selection of a potential 5′ splice site and additional RNA or protein factors have to be invoked. An example of a protein splicing factor, ASF/SF2, that is involved in the association of U1 snRNP with the pre-mRNA has recently been reported (44).

A role for U5 snRNA (16,17,19) and U6 snRNA (19,45–47) in the recognition of 5′ cleavage sites has been suggested. We have therefore compared the base complementarity of U5 snRNA with exon and intron sequences at the regular and cryptic 5′ splice sites, and of U6 snRNA with intron sequences at both sites. This did not reveal differences that can account for the selection of the regular site and the silencing of the cryptic site under normal growth conditions.

Since neither U1 nor U5 and U6 snRNAs appear to be sufficient for the definition of a 5′ splice site, it is plausible that a heat-labile factor is involved in directing the cleavage to a particular 5′ splice site. Two simple modes of action are possible for this putative factor. The factor could be an activator of splicing, that under normal growth conditions ensures that only normal splice sites are selected for cleavage and subsequent

ligation. Upon heat treatment, the factors specificity is altered, thus permitting it to interact with more putative splice sites in a less discriminating manner. Alternatively, the factor could function as a repressor. Under normal growth conditions, it would associate with the cryptic 5′ splice sites and prevent its cleavage. At elevated temperatures, the affinity of the factor to the cryptic site would be reduced and its dissociation render the consensus cryptic site available for cleavage.

Whichever of the above mechanisms is responsible for the silencing of the cryptic site under normal growth conditions, it cannot account for our observation that even after the block to cleavage is alleviated by heat shock, splicing at the cryptic site does not proceed to completion by ligation to a proximal downstream 3′ exon. The absence of ligation at the cryptic splice site may be due to a heat-induced general perturbation to factor(s) required for the second step of splicing (48). However, it is possible that the splicing machinery recognizes sequences at the cryptic exon as aberrant, and therefore does not proceed with the second step of splicing. The existence of such a mechanism is compatible with previous studies showing that the introduction of nonsense mutations *in vivo* resulted in low levels of the mutated mRNAs (49–54). Nonsense mutations were thus proposed to affect RNA processing by either a translation translocation (50,54) or a nuclear scanning mechanism (50). In our case, examination of the intron sequence upstream to the cryptic site reveals two stop codons that are in frame with the 5′ exon. We therefore propose a 'checking mechanism' as part of the splicing machinery, which detects the presence of an open reading frame from the first AUG to the end of the pre-mRNA. The 'checking mechanism' can operate before each step of the splicing reaction. When an in-frame stop codon is identified upstream to a legitimate putative 5′ splice site, splicing at this site is aborted. This mechanism may explain the exclusion of the cryptic site under normal growth conditions. When cleavage at the cryptic site occurs after heat shock, we observe that the second step of splicing is blocked at the cryptic site, suggesting that once a stop codon is introduced into an intermediate exon, splicing can still be aborted before the second step, thus preventing the production of a defective message.

## ACKNOWLEDGEMENTS

We are greatly indebted to Dr Shoshana Klein for her invaluable advice and helpful suggestions in writing the manuscript. We thank Mina Angenitzki for her assistance with the electron microscopy. This work was supported in part by grants from the Leo and Julia Forchheimer Center for Molecular Genetics at the Weizmann Institute of Science, the Basic Research Foundation of the Israel Academy of Sciences, and the US–Israel Binational Science Foundation to J.S., and a grant from the US–Israel Binational Science Foundation to R.S.

## REFERENCES

1. Green, M.R. (1991) *Annu. Rev. Cell Biol.*, **7**, 559–599.
2. Moore, J.M., Query, C.C., and Sharp, P.A. (1993) In Gesteland, R.F., and Atkins, J.F. (ed.), The RNA World. Cold Spring Harbor Laboratory Press, Cold Spring Harbor, New York, pp. 303–358.
3. Krainer, A.R., and Maniatis, T. (1988) In Hames, B.D., and Glover, D.M. (ed.), Transcription and Splicing. IRL Press, Oxford, pp. 131–206.
4. Steitz, J.A., Black, D.L., Gerke, V., Parker, K.A., Kramer, A., Frendewey, D., and Keller, W. (1988) In Birnstiel, M.L. (ed.), Structure and Function of Major and Minor Small Nuclear Ribonucleoprotein Particles. Springer-Verlag, Heidelberg, pp. 115–154.
5. Kretzner, L., Rymond, B.C., and Rosbash, M. (1987) *Cell*, **50**, 593–602.
6. Séraphin, B., Kretzner, L., and Rosbash, M. (1988) *EMBO J.*, **7**, 2533–2538.
7. Séraphin, B., and Rosbash, M. (1990) *Cell*, **63**, 619–629.
8. Siliciano, P.G., and Guthrie, C. (1988) *Genes Dev*, **2**, 1258–1267.
9. Aebi, M., Hornig, H., and Weissmann, C. (1987) *Cell*, **50**, 237–246.
10. Weber, S., and Aebi, M. (1988) *Nucleic Acids Res.*, **16**, 471–486.
11. Eperon, L.P., Estibeiro, J.P., and Eperon, I.C. (1986) *Nature (London)*, **324**, 280–282.
12. Lear, A.L., Eperon, L.P., Wheatley, I.M., and Eperon, I.C. (1990) *J. Mol. Biol.*, **211**, 103–115.
13. Nelson, K.K., and Green, M.R. (1988) *Genes Dev.*, **2**, 319–329.
14. Ohshima, Y., and Gotoh, Y. (1987) *J. Mol. Biol.*, **195**, 247–259.
15. Green, M.R. (1986) *Annu.Rev.Genet.*, **20**, 671–708.
16. Newman, A.J., and Norman, C. (1991) *Cell*, **65**, 115–123.
17. Newman, A.J., and Norman, C. (1992) *Cell*, **68**, 743–754.
18. Sawa, H., and Shimura, Y. (1992) *Genes Dev.*, **6**, 244–254.
19. Wassarman, D.A., and Steitz, J.A. (1992) *Science*, **257**, 1918–1925.
20. Yost, H.J., and Lindquist, S. (1986) *Cell*, **45**, 185–193.
21. Yost, H.J., and Lindquist, S. (1988) *Science*, **242**, 1544–1548.
22. Yost, H.J., and Lindquist, S. (1991) *Mol. Cell. Biol.*, **11**, 1062–1068.
23. Muhich, M.L., and Boothroyd, J.C. (1988) *Mol. Cell. Biol.*, **8**, 3837–3846.
24. Maniak, M., and Nellen, W. (1988) *Mol. Cell. Biol.*, **8**, 153–159.
25. Bond, U., and Schlesinger, M.J. (1986) *Mol. Cell. Biol.*, **6**, 4602–4610.
26. Bond, U. (1988) *EMBO J.*, **7**, 3509–3518.
27. Yost, H.J., Petersen, R.B., and Lindquist, S. (1990) *Trends Genet*, **6**, 223–227.
28. Spann, P., Feinerman, M., Sperling, J., and Sperling, R. (1989) *Proc. Natl. Acad. Sci. USA*, **86**, 466–470.
29. Sperling, R., Sperling, J., Levine, A.D., Spann, P., Stark, G.R., and Kornberg, R.D. (1985) *Mol. Cell. Biol.*, **5**, 569–575.
30. Ast, G., Goldblatt, D., Offen, D., Sperling, J., and Sperling, R. (1991) *EMBO J.*, **10**, 425–432.
31. Sperling, R., Spann, P., Offen, D., and Sperling, J. (1986) *Proc. Natl. Acad. Sci. USA*, **83**, 6721–6725.
32. Sperling, R., and Sperling, J. (1990) In Strauss, P.R., and Wilson, S.H. (ed.), The Eukaryotic Nucleus, Molecular Biochemistry and Macromolecular Assemblies. Telford Press, Caldwell, NJ, pp. 453–476.
33. Padgett, R.A., Wahl, G.M., and Stark, G.R. (1982) *Mol. Cell. Biol.*, **2**, 293–301.
34. Kempe, T.D., Swyryd, E.A., Bruist, M., and Stark, G.R. (1976) *Cell*, **9**, 541–550.
35. Zieg, J., Clayton, C.E., Ardeshir, F., Giulotto, E., Swyryd, E.A., and Stark, G.R. (1983) *Mol. Cell. Biol.*, **3**, 2089–2098.
36. Chirgwin, J.M., Przbyla, A.E., MacDonald, R.J., and Rutter, W.J. (1979) *Biochemistry*, **18**, 5294–5299.
37. Lührmann, R. (1988) In Birnstiel, M.L. (ed.), Structure and Function of Major and Minor Small Nuclear Ribonucleoprotein Particles. Heidelberg, pp. 71–96.
38. Kay, R.J., Russnak, R.H., Jones, D., Mathias, C., and Candido, E.P.M. (1987) *Nucleic Acids Res.*, **15**, 3723–3741.
39. Shukla, R.R., Dominski, Z., Zwierzynski, T., and Kole, R. (1990) *J. Biol. Chem.*, **265**, 20377–20383.
40. Utans, U., Behrens, S., Lührmann, R., Kole, R., and Kramer, A. (1992) *Genes Dev.*, **6**, 631–641.
41. Mayrand, S., and Pederson, T. (1983) *Mol. Cell. Biol.*, **3**, 161–171.
42. Kloetzel, P.M., and Bautz, E.K.F. (1983) *EMBO J.*, **2**, 705–710.
43. Kloetzel, P.M., and Schuldt, C. (1986) *Biochim.Biophys.Acta.*, **867**, 9–15.
44. Kohtz, J.D., Jamison, S.F., Will, C.L., Zuo, P., Lührmann, R., Garcia-Blanco, M.A., and Manley, J.L. (1994) *Nature (London)*, **368**, 119–124.
45. Lesser, C.F., and Guthrie, C. (1993) *Science*, **262**, 1982–1988.
46. Kandels-Lewis, S., and Séraphin, B. (1993) *Science*, **262**, 2035–2039.
47. Sontheimer, E.J., and Steitz, J.A. (1993) *Science*, **262**, 1989–1996.
48. Krainer, A.R., and Maniatis, T. (1985) *Cell*, **42**, 725–736.
49. Baserga, S.J., and Benz, E.J. (1988) *Proc. Natl. Acad. Sci. USA*, **85**, 2056–2060.
50. Urlaub, G., Mitchell, P.J., Ciudad, C.J., and Chasin, L.A. (1989) *Mol. Cell. Biol.*, **9**, 2868–2880.
51. Naeger, L.K., Schoborg, R.V., Zhao, Q., Tullis, G.E., and Pintel, D.J. (1992) *Genes Dev.*, **6**, 1107–1119.
52. Belgrader, P., Cheng, J., and Maquat, L.E. (1993) *Proc. Natl. Acad. Sci. USA*, **90**, 482–486.
53. Cheng, J., and Maquat, L.E. (1993) *Mol. Cell. Biol.*, **13**, 1892–1902.
54. Daar, I.O., and Maquat, L.E. (1988) *Mol. Cell. Biol.*, **8**, 802–813.